Regular Article

Sonosynthesis of Thiazolidinones Using Nano-Fe₃O₄-tethered Polyhedral Oligomeric Silsesquioxanes with Eight Branches of 3-Aminopropyltriethoxysilane

J. Safaei-Ghomi[a,*], S.H. Nazemzadeh[a], M. Alnasrawi[b] and H. Shahbazi-Alavi[a]

[a]*Department of Organic Chemistry, Faculty of Chemistry, University of Kashan, Kashan, P. O. Box: 87317-51167, I. R.Iran*
[b]*Department of Inorganic Chemistry, Faculty of Chemistry, University of Kashan, Kashan,IR, Iran*

An effective way for the synthesis of *bis*-thiazolidinones was applied by one-pot pseudo-five-component reaction of benzaldehydes, ethylenediamine, 2-mercaptoacetic acid with nano-Fe₃O₄-tethered polyhedral oligomeric silsesquioxanes with eight branches as catalyst under ultrasonic conditions. The catalyst was characterized by Fourier-transform infrared spectroscopy, scanning electron microscope, X-ray diffraction, energy-dispersive X-ray spectroscopy, Brunauer-Emmett-Teller, thermogravimetric analysis, and vibrating-sample magnetometer. The remarkable advantages of this methodology are easy work-up, short reaction times, high to excellent product yields, low catalyst loading and reusability of the catalyst.

INTRODUCTION

Thiazolidinones represent biological properties including anticancer [1], anti-virus [2], antibacterial [3], antituberculous therapy [4] and anti-AIDS [5] activities. These activities make them attractive targets in organic synthesis. Therefore, seeking easy and brief techniques for the preparation of thiazolidinones could be a significant subject. Among the thiazolidine derivatives, *bis*-thiazolidinones have received substantial attention because of their biologic activity [6-7]. Recently, reports have been developed on synthesis of *bis*-thiazolidinones using the catalysts such as Zeolite [8], $HClO_4$-SiO_2 [9], ChCl (Choline Chloride)/urea based ionic liquid) [10] and $ZnCl_2$ [11]. Despite the use of these ways, there remains adequate purpose to offer a new way for an efficient, high yielding, and mild approach to achieve such systems. Ideally, utilizing environmental and green catalysts which can be simply recycled at the end of reactions has obtained significant attention in recent years [12-15]. Recently,

performing one-pot reactions with a nanocatalyst under ultrasonic irradiation has been given much attention [16-17]. The ultrasound approach decreases time, and increases yields by creating the activation energy in micro surroundings [18-19]. Cavitation process generates high temperature and pressure in the micro surroundings which disturbs the current in the liquid and elevated mass transfer [20-21]. Recently, several nano-catalysts have been utilized for the preparation of organic compounds under ultrasonic conditions [22-23]. The surface of magnetic nanoparticles (MNPs) can be modified through loading by desirable functionalities such as polyhedral oligomericsilsesquioxanes (POSS). Silsesquioxane is an organosilicon compound with the chemical formula $[RSiO_{3/2}]_n$ (R = H, alkyl, vinyl, aryl, alkoxy) [24,25]. In continuation of our works on synthesis of magnetic nanoparticles [26,28], a polyhedral oligomeric silsesquioxanes with eight triethoxysilane branches (APTPOSS) has been anchored on the surface of Fe₃O₄ nanomagnetics. In the current study, we investigated an easy and rapid method for the synthesis of *bis*-thiazolidinones by one-pot pseudo-five-component reaction of benzaldehydes, ethylenediamine and 2-mercaptoacetic acid using

_____

*Corresponding author. E-mail: safaei@kashanu.ac.ir
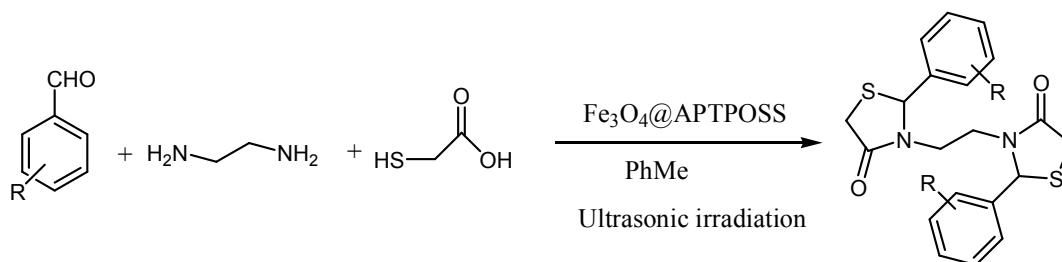
Scheme 1. Synthesis of *bis*-thiazolidinones using nano-Fe$_3$O$_4$@APTPOSS under ultrasonic irradiation

nano-Fe$_3$O$_4$@APTPOSS as reusable catalyst under ultrasonic conditions (Scheme 1).

EXPERIMENTAL

Preparation of Nano-Fe$_3$O$_4$

Magnetic nano-Fe$_3$O$_4$ was prepared *via* improved chemical co-precipitation process [29].

Preparation of Cl-POSS

Starting material octakis(3-chloropropyl)octasilsesquioxane was prepared according to the literature [30-33].

Preparation of Octakis[3-(3-aminopropyl triethoxysilane) Propyl] Octasilsesquioxane

Firstly, 2 mmol (2.07 g) of Cl-POSS was added to 20 mmol (4.43 g) of 3-aminopropyltriethoxysilane and the mixture was transferred to a round-bottom flask under N$_2$ atmosphere. The mixture was heated in an oil bath at 110 ºC for 2 days. After completion of the reaction, the mixture was cooled to room temperature and the mixture was filtered and washed with acetone and methanol to remove the additional reactants. Finally, the resultant pale brown precipitates were dried in a vacuum oven at 70 °C for 12 h.

Preparation of Nano-Fe$_3$O$_4$@APTPOSS

1.10 g of magnetic Fe$_3$O$_4$ nanoparticles was added to 30 ml of ethanol and sonicated at 35 W power for 30 min to completely dispersed. Afterward 0.40 g APTPOSS and 1.6 ml NH$_4$OH were sonicated at 25 W power in a mixture of 20 ml water and 40 ml ethanol for 1h. Then, the reaction mixture was maintained at 80 °C and then the Fe$_3$O$_4$ suspension was slowly added dropwise for 90 min. The

reaction was carried out for a further 3 days to reach completion (Scheme 2). Finally, the resulting product was filtered by an external magnet and washed with distilled water and acetone several times and dried at 60 ºC for 12 h in vacuum to afford pure Fe$_3$O$_4$@APTPOSS MNPs.

General Procedure for the Preparation of Bis-thiazolidinones

A mixture of aldehydes (2 mmol), ethylenediamine (1 mmol), 2-mercaptoacetic acid (2 mmol) and 6 mg of nano-Fe$_3$O$_4$@APTPOSS in PhMe (20 ml) was sonicated at 40 W power. After completion of the reaction (monitored by TLC), the nanocatalyst was easily separated using an external magnet. The crude mixture of isomers was separated by silica gel column chromatography (diethyl ether/petroleum ether in variable ratio mixtures). In general *meso* isomers eluted more slowly than corresponding racemates. The *racemate* isomers were obtained in higher yields than *meso* isomers. The yields of the racemate isomers are presented in Table 2.

RESULTS AND DISCUSSION

Structural Analysis of Nano-Fe$_3$O$_4$@APTPOSS

The systematic steps of magnetite nanoparticle (Fe$_3$O$_4$)@octakis[3-(3-aminopropyltri ethoxysilane)propyl] octasilsesquioxane (APTPOSS) preparation are described in scheme 2. In the first step, magnetic iron oxide nanoparticles were synthesized by co-precipitation Fe(II) and Fe(III) ions in basic solution. Then, Cl-POSS was synthesized by the hydrolysis of 3-chloropropyltrimethoxysilane under acidic conditions. The reaction of 3-aminopropyltriethoxysilane with Cl-POSS gave APTPOSS. Treatment of naked-Fe$_3$O$_4$ with POSS derivative afforded
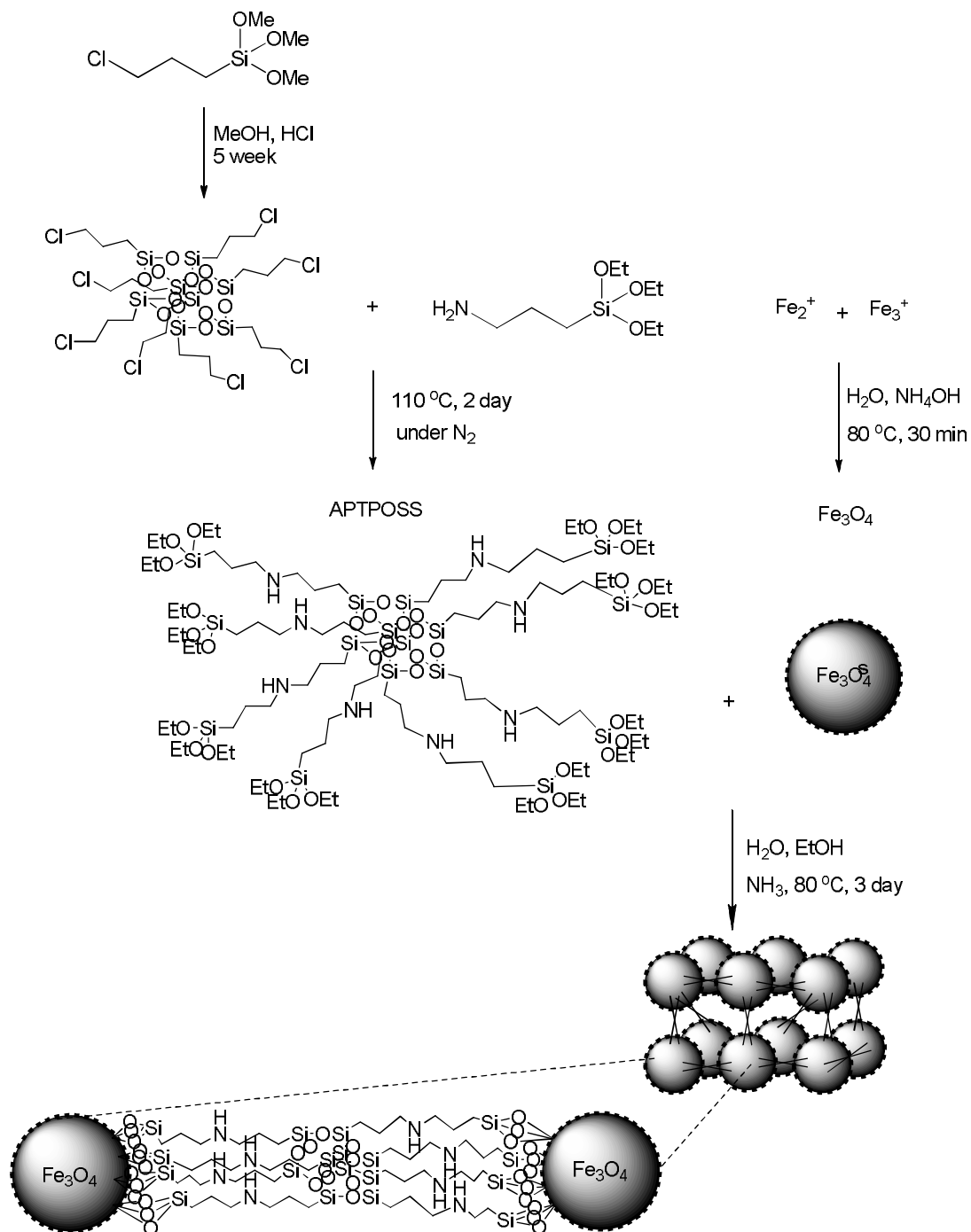
Scheme 2. Preparation routes of nano-Fe$_3$O$_4$@APTPOSS

Fe$_3$O$_4$@APTPOSS MNPs.

Figure 1 displays the Fourier transform infrared (FTIR) spectra of Fe$_3$O$_4$ MNPs, Cl-POSS, APTPOSS and Fe$_3$O$_4$@APTPOSS. The O-H bending vibration near 1631 cm^{-1} and Fe-O stretching vibration near 584 cm^{-1} were observed for Fe$_3$O$_4$@APTPOSS and Fe$_3$O$_4$ in Figs. 1a and
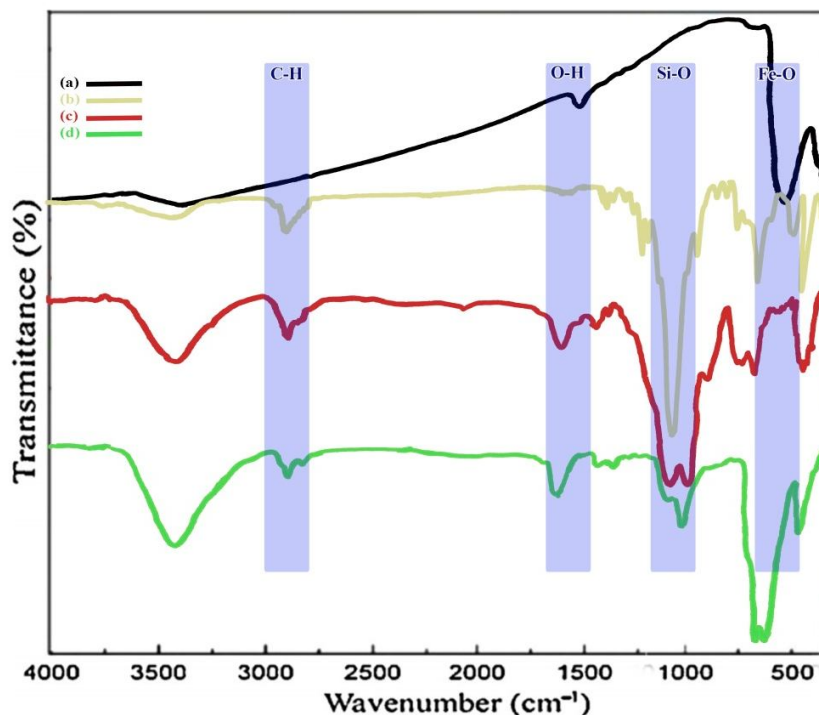
Fig. 1. FT-IR spectra for (a) Fe_3O_4, (b) Cl-POSS (c) APTPOSS and (d) Fe_3O_4@APTPOSS.

d. Figure 1b shows the presence of the peaks at 810 cm^{-1} (C-Cl stretching), 1104 (Si-O stretching) and 2954 cm^{-1} (-CH$_2$ stretching) which confirm the presence of Cl-POSS. The appearance of linker to the surface of Fe_3O_4 MNPs is proved by the bands at about 691 cm^{-1} (Si-O bending), 1021-1151 cm^{-1} (Si-O stretching) and 2910-2970 cm^{-1} (C-H stretching). These peaks were observed for APTPOSS and Fe_3O_4@APTPOSS in Figs. 1c and d.

Figure 2 shows the XRD patterns of Fe_3O_4 MNPs, APTPOSS and Fe_3O_4@APTPOSS. X-ray diffraction patterns of Figs. 2b and c show a cubic iron oxide phase ($2\theta = 30.16°, 36.11°, 43.46°, 54.12°, 57.52°, 62.98°$). The broad peaks at 2θ from $16°$ to $28°$ shown for APTPOSS and Fe_3O_4@APTPOSS are ascribed to amorphous silicon-oxygen bonds.

The magnetization curves of Fe_3O_4 and the catalyst are shown in Fig. 3. The magnetization of iron oxide particles and Fe_3O_4@APTPOSS at room temperature was found to be about 64 and 42 emu g^{-1}, respectively. This difference indicates that the Fe_3O_4 MNPs were loaded into APTPOSS

in Fe_3O_4@APTPOSS MNPs.

We considered the dynamic light scattering of magnetic nanocatalyst in deionized water in Fig. 4. The DLS results indicated the size distribution from the correlation function. Since the naked Fe_3O_4 are attached to each other by APTPOSS to form the final three-dimensional architectures, dynamic light scattering can serve as an effective device to monitor this behavior. Based on the DLS results, it could be concluded that 3-D Fe_3O_4@APTPOSS MNPs have been successfully prepared.

Figure 5 shows energy dispersive spectroscopy (EDS) of Fe_3O_4, APTPOSS and Fe_3O_4@APTPOSS. The EDS results showed the presence of Fe, N, O, C and Si in the nanomagnetic-supported organic-inorganic hybrids based on POSS, indicating that the Octakis[3-(3-aminopropyl-triethoxysilane)propyl]octasilsesquioxanes have been incorporated in the MNPs coating. Also, the lower intensity of Fe peaks compared with Si peak shows magnetic Fe_3O_4 nanoparticles were trapped by APTPOSS.
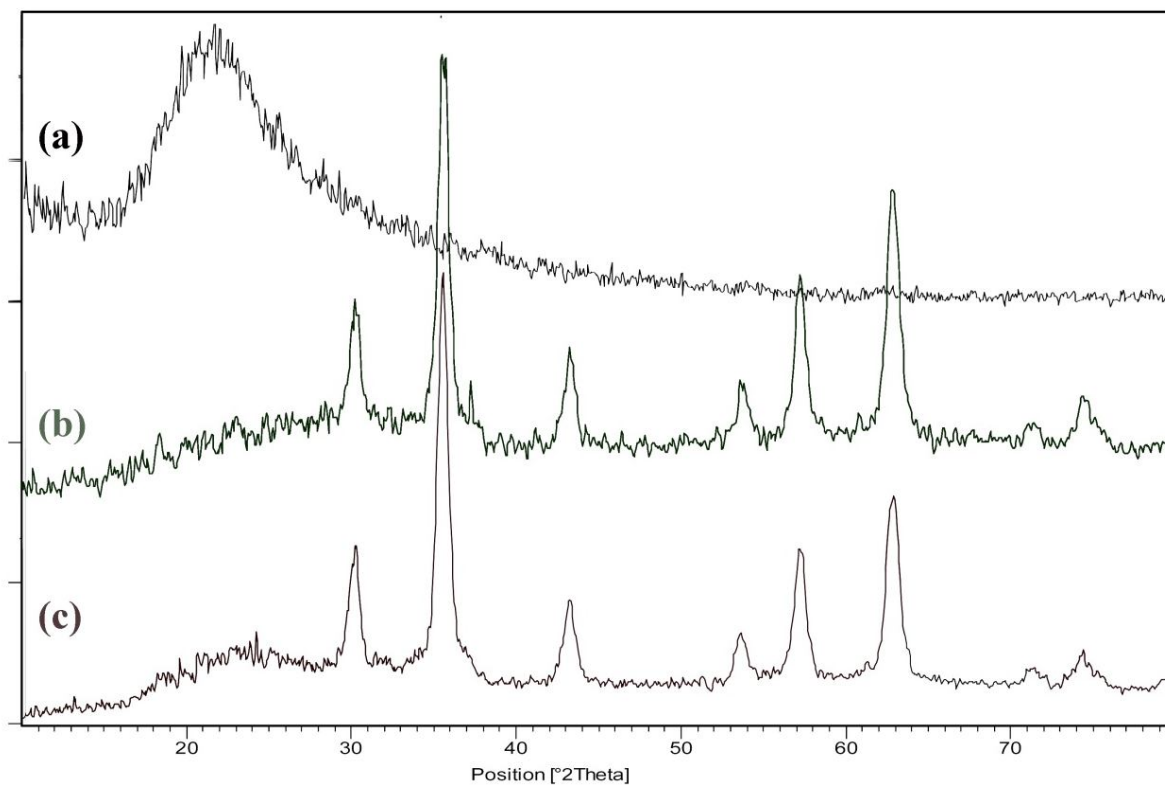
The thermal stability of the Fe_3O_4@APTPOSS was

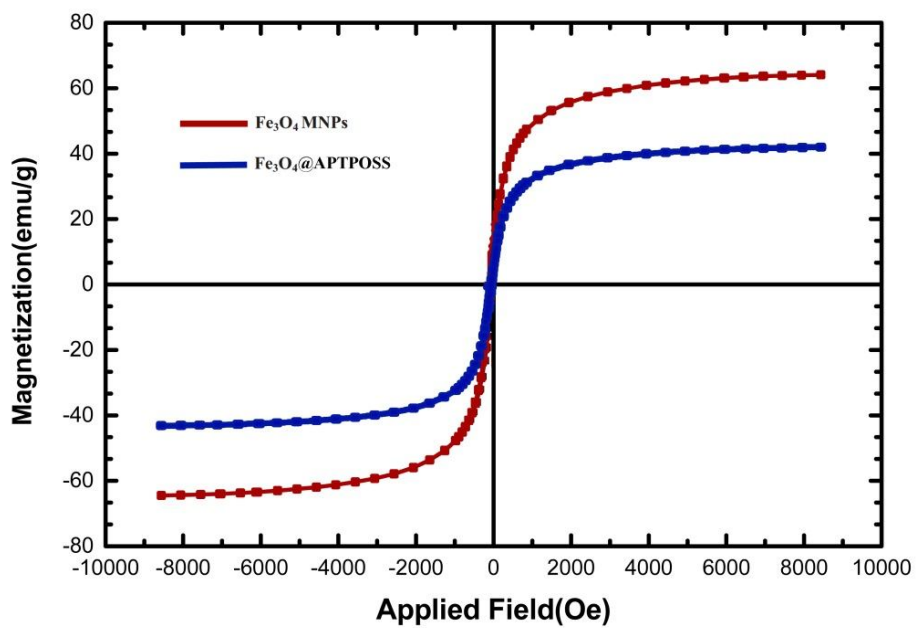**Fig. 2.** XRD patterns of (a) APTPOSS, (b) Fe_3O_4 and (c) Fe_3O_4@APTPOSS.

Fig. 3. Magnetization curves for the prepared Fe_3O_4 and Fe_3O_4@APTPOSS.
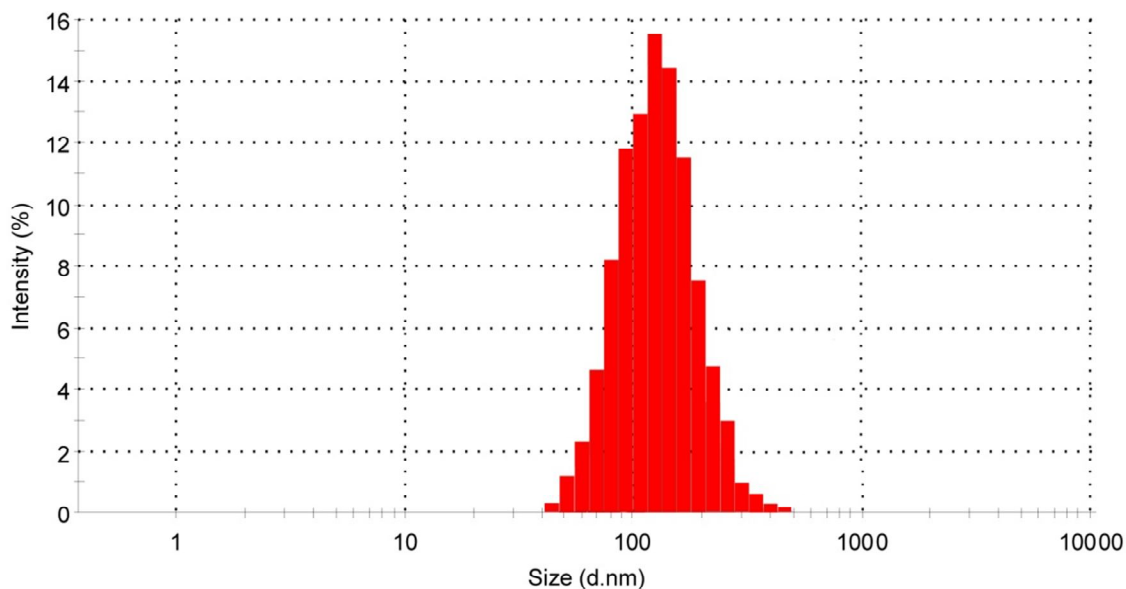
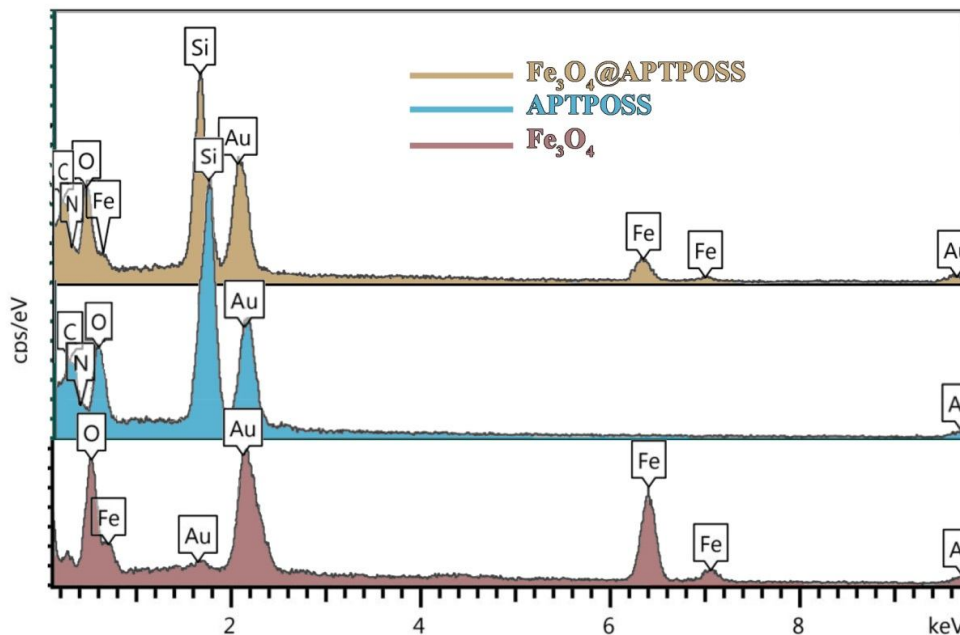**Fig. 4.** Dynamic laser scattering of Fe_3O_4@APTPOSS.

Fig. 5. Comparison of energy dispersive spectroscopy spectra for Fe_3O_4, APTPOSS and Fe_3O_4@APTPOSS.

investigated by thermogravimetric analysis. The TGA curve of the magnetic nanocatalyst shows the mass loss of the organic compounds as it decomposes upon heating (Fig. 6).

The initial weight loss from the catalyst below 220 °C is assigned to the loss of the physically adsorbed solvents. The next TGA peak is a weight loss of 14% at about 220-750 °C
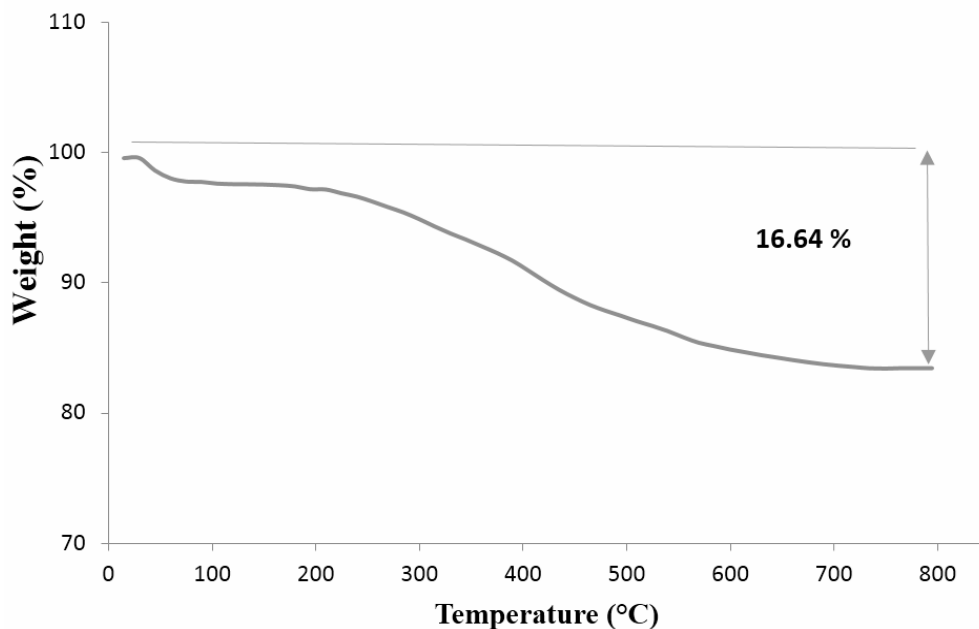
Fig. 6. TGA curve of Fe_3O_4@APTPOSS MNPs.

that is attributed to the decomposition of the organic species. Hence, Fe_3O_4@APTPOSS was stable up to 220 °C. Fig. 6

Figure 7 depicts the FE-SEM images of magnetic nanoparticles without and with APTPOSS. The size of the Fe_3O_4 seeds and Fe_3O_4@APTPOSS are around 22 and 130 nm, respectively, indicating that the POSS-based inorganic/organic hybrid is successfully anchored to the Fe_3O_4 particles.

The BET specific surface area of Fe_3O_4 and Fe_3O_4@APTPOSS nanoparticles was measured by the nitrogen gas adsorption-desorption isotherms (Fig. 8). The results presented that the BET specific surface area of Fe_3O_4 was improved from 10.15 to 28.12 $m^2 g^{-1}$ after modification with APTPOSS, therefore more active sites were introduced on nano-Fe_3O_4@APTPOSS surface.

Synthesis of Bis-thiazolidinones Using Nano-Fe_3O_4@APTPOSS as Catalyst

At first, we investigated the different catalysts for the model reaction of 4-chlorobenzaldehyde (2 mmol), ethylenediamine (1 mmol), 2-mercaptoacetic acid (2 mmol) in diverse solvents. The model reaction was checked using various catalysts including nano-CeO_2, nano-SnO, nano-

Fe_3O_4, APTPOSS and nano-Fe_3O_4@APTPOSS. We optimized different conditions and found that the reaction gave satisfying result in the presence of nano-Fe_3O_4@APTPOSS (6mg) under ultrasonic conditions (40 W) in toluene (Table 1). Turnover frequency (TOF) of different catalysts was calculated in Table 1. The result showed that the Fe_3O_4@APTPOSS is more effective than other catalyst.

With these promising results in hand, we then explored the possibility of the reaction using various aromatic aldehydes as substrates. The results show the present catalytic method is extensible to a wide diversity of substrates to create a variety-oriented library of *bis*-thiazolidinones (Table 2).

We also checked reusability of Fe_3O_4@APTPOSS as a nanomagnetic catalyst; its reusability was achieved by the reaction of *p*-Cl-benzaldehyde (2 mmol), ethylenediamine (1 mmol), 2-mercaptoacetic acid (2 mmol) and 6 mg of nano-Fe_3O_4@APTPOSS under optimized conditions. After completion of the reaction, the catalyst was washed with water and acetone, dried in an oven at 80 °C for 100 min and used with new substrates under the same conditions. The results showed that the MNPs-supported POSS can be reused several times (Fig. 9).
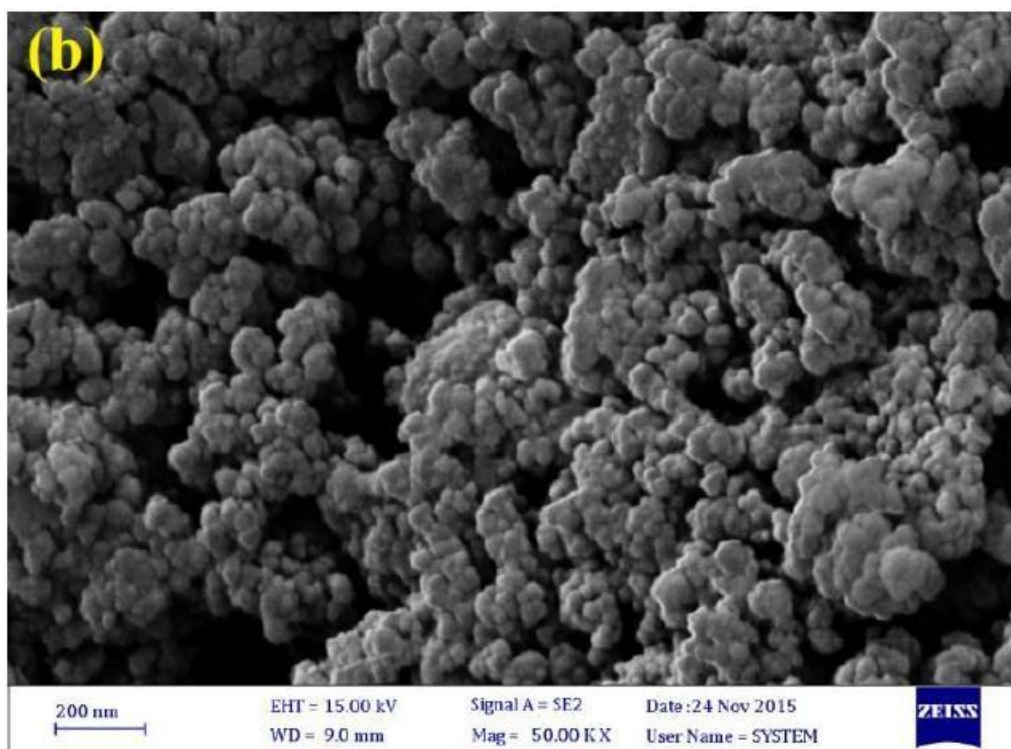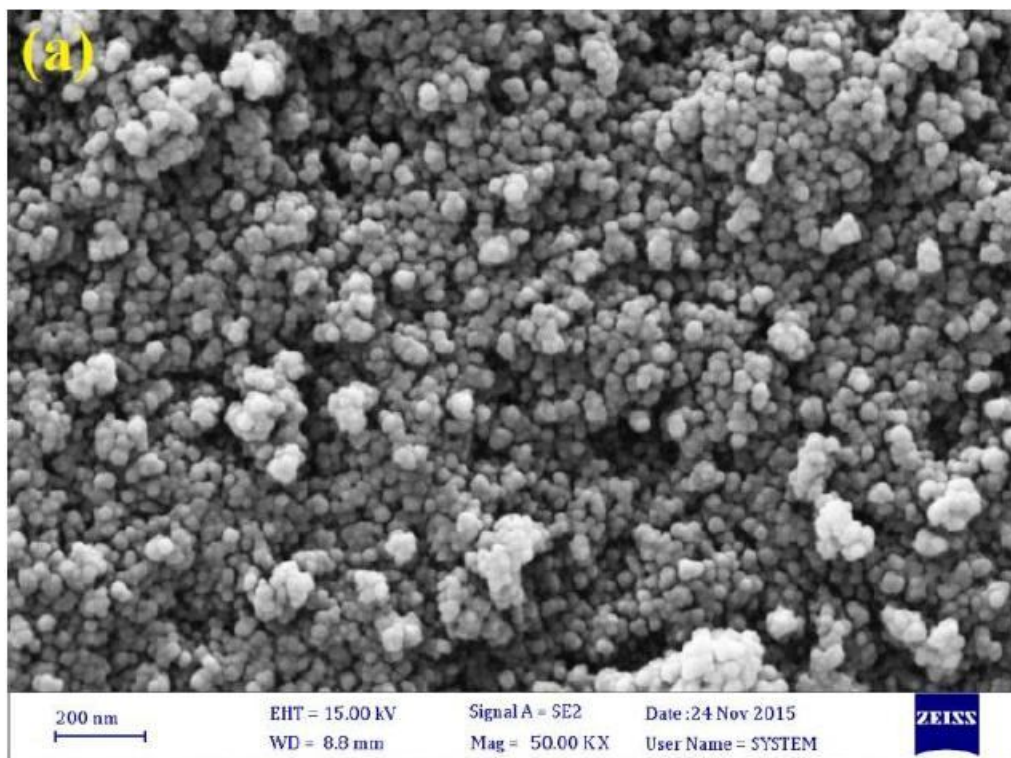
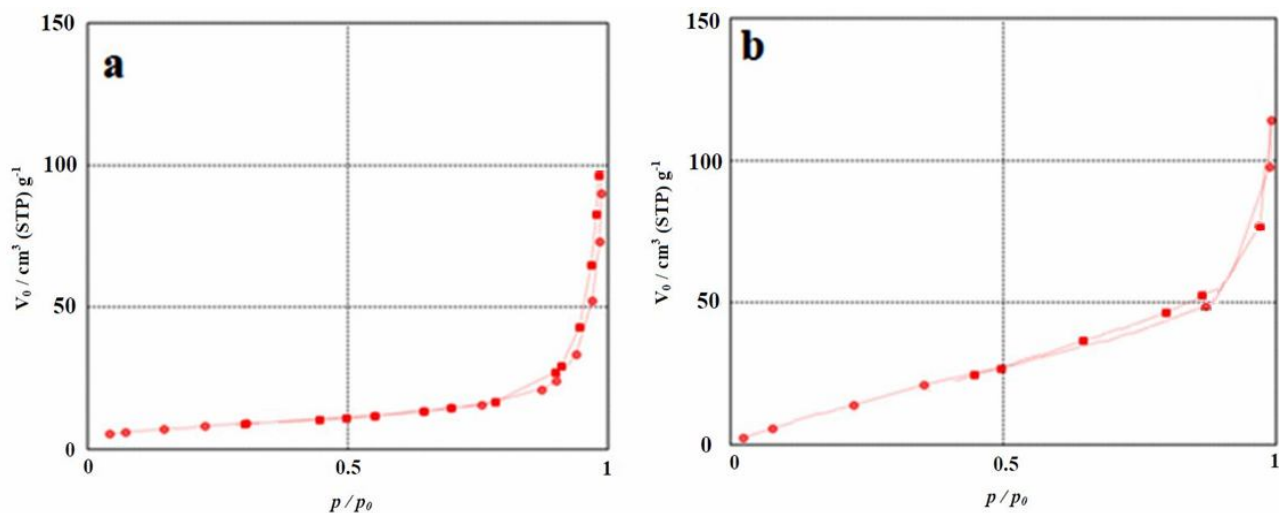**Fig. 7.** SEM images of (a) Fe_3O_4 and (b) Fe_3O_4@APTPOSS.

Fig. 8. The BET specific surface area of (a) Fe_3O_4 and (b) Fe_3O_4@APTPOSS.

Table 1. The Model Reaction was Checked by Diverse Catalysts[a]

Entry	Solvent	Catalyst (mg)	Time (min)	Yield (%)[b]	TOF (min^{-1})
1	Toluene (Reflux)	No catalyst	300	<10	
2	DMF (Reflux)	CeO$_2$ NPs (20)	240	34	0.12
3	Toluene (Reflux)	CeO$_2$ NPs (20)	240	37	0.14
4	Toluene (Reflux)	SnO NPs (20)	240	39	0.16
5	Toluene (Reflux)	Fe$_3$O$_4$ MNPs (10)	240	30	0.10
6	Toluene (Reflux)	Fe$_3$O$_4$ MNPs (20)	240	30	0.10
7	Toluene (Reflux)	APTPOSS (10)	140	43	0.22
8	DMF (Reflux)	Nano-Fe$_3$O$_4$@APTPOSS (10)	120	67	0.66
9	EtOH (Reflux)	Nano-Fe$_3$O$_4$@APTPOSS (10)	120	48	0.50
10	CH$_3$CN (Reflux)	Nano-Fe$_3$O$_4$@APTPOSS (10)	120	56	0.58
11	Toluene (Reflux)	Nano-Fe$_3$O$_4$@APTPOSS(6)	120	71	0.74
12	Toluene (Reflux)	Nano-Fe$_3$O$_4$@APTPOSS (10)	120	75	0.80
13	Toluene (Reflux)	Nano-Fe$_3$O$_4$@APTPOSS (14)	120	75	0.80
14	Toluene (US)[c]	Nano-Fe$_3$O$_4$@APTPOSS (4)	15	82	6.52
15	Toluene (US)[c]	Nano-Fe$_3$O$_4$@APTPOSS (6)	15	86	6.84
16	Toluene (US)[c]	Nano-Fe$_3$O$_4$@APTPOSS (8)	15	86	6.84
17	Toluene (US)[c]	-	30	60	2.42

[a]4-Chlorobenzaldehyde (2 mmol), ethylenediamine (1 mmol), 2-mercaptoacetic acid (2 mmol). [b]Isolated yields. [c]Ultrasonic irradiation (40 W).

Table 2. Preparation of *Bis*-thiazolidinones Using Nano-Fe$_3$O$_4$@APTPOSS under Ultrasonic Irradiation

Entry	Aldehyde	Product	Time (min)	Yield (%)[a]	m. p. (°C) [Ref.]	m. p (°C)
1	4-Cl-C$_6$H$_4$	4a	15	86	285-288 [34]	150-152
2	2-Cl-C$_6$H$_4$	4b	20	80	210-211 [34]	143-145
3	C$_6$H$_5$	4c	15	80	152-155 [9]	155-157
4	4-NO$_2$-C$_6$H$_4$	4d	15	84	-	164-166
5	3-NO$_2$-C$_6$H$_4$	4e	20	79	-	222-224
6	Pyridin-2-yl	4f	20	78	167-169 [35]	170-172
7	Pyridin-3-yl	4g	20	76	198-200 [35]	191-193
8	Pyridin-4-yl	4h	20	74	224-225 [35]	221-223
9	4-CH$_3$-C$_6$H$_4$	4i	15	81	-	158-160
10	4-Isopropyl-C$_6$H$_4$	4j	25	75	-	163-165

[a]Isolated yields.
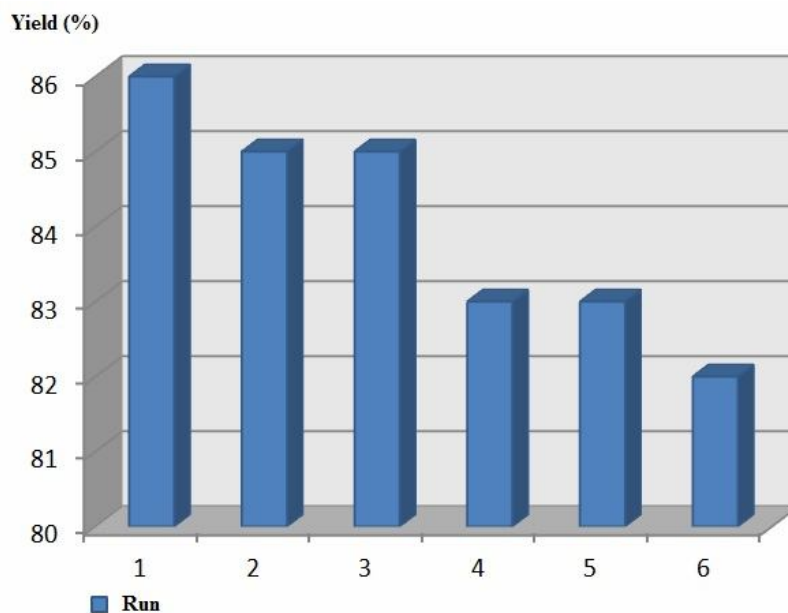
Fig. 9. Reusability of MNPs@APTPOSS for the preparation of 4a**.**

To compare the efficiency of nano-Fe$_3$O$_4$@APTPOSS with the reported catalysts for the synthesis of *bis*-thiazolidine, we have tabulated the results in Table 3. As indicated in Table 3, nano-Fe$_3$O$_4$@APTPOSS is superior with respect to the reported catalysts in terms of reaction time, yield and conditions. As expected, the increased

Table 3. Comparison of Catalytic Activity of Nano-Fe_3O_4@APTPOSS with other Reported Catalysts for Synthesis 4a

Entry	Catalyst (condition)	Time (min)	Yield (%)[a]	[Ref.]
1	$HClO_4$-SiO_2 (2.5 mmol) (10 mol%, PhMe, 100 °C)	360	62	[9]
2	(Choline chloride)/urea based ionic liquid) (10 mol%, 80 °C)	240	79	[10]
3	$ZnCl_2$ (5 mol%, PhMe, 110 °C)	20	81	[11]
4	Nano-Fe_3O_4@APTPOSS (6 mg, toluene, ultrasonic irradiation, 40 W)	15	86	This work

[a]Isolated yield.

surface area due to small particle size increased reactivity of catalyst. This factor is responsible for the accessibility of the substrate molecules on the catalyst surface.

The Proposed Reaction Mechanism

A probable mechanism for the synthesis of *bis*-thiazolidine derivatives using MNPs@APTPOSS is shown in Scheme 3. It is assumed that catalytically active site of catalyst contains Fe_3O_4 (Fe^{3+}) that acts as a Lewis acid and APTPOSS (-NH-) that acts as a Lewis base. Therefore, Fe_3O_4 is coordinated to the carbonyl groups of aldehydes, and APTPOSS interacts with acidic protons. A proposed mechanism is outlined *via* primary imine intermediate formation followed by attack of the sulfur atoms of 2-mercaptoacetic acid on the activated imine groups followed by intramolecular cyclization with the elimination of H_2O giving rise to the cyclized product *bis*-thiazolidines. The amino groups distributed on the surface of MNPs@APTPOSS activate the groups of the substrates through hydrogen bonding [26-27].

CONCLUSIONS

Currently, using the ultrasonic and nanoparticles-supported inorganic-organic hybrids, based on POSS, as a combined catalytic system, is a highly efficient protocol for the synthesis of *bis*-thiazolidines. The advantages of this new procedure are high yields in short reaction times, operational simplicity, several reuse times without

significant losses in performance and ease of recovery from the reaction mixture *via* application of an external magnetic. Therefore, this method can be used as a replacement for conventional thermal system for the preparation of a wide range of *bis*-thiazolidines.

REFERENCES

[1] K. Appalanaidu, R. Kotcherlakota, T.L. Dadmal, V.S. Bollu, R.M. Kumbhare, C.R. Patra, Bioorg. Med. Chem. Lett. 26 (2016) 5361.

[2] V. Ravichandran, A. Jain, K.S. Kumar, H. Rajak, R.K. Agrawal, Chem. Biol. Drug. Des. 78 (2011) 464.

[3] A.K. Kulkarni, V.H. Kulkarni, J. Keshavayya, V.I. Hukkeri, H.W. Sung, Macromol. Biosci. 5 (2005) 490.

[4] B.M. Mistry, S. Jauhari, Med. Chem. Res. 22 (2013) 635.

[5] V. Ravichandran, B.R.P. Kumar, S. Sankar, R.K. Agrawal, Eur. J. Med. Chem. 44 (2009) 1180.

[6] W.A.A. Arafa, M.G. Badry, J. Chem. Res. 40 (2016) 385.

[7] K.M. Dawood, H.K.A. Abu-Deif, Eur. J. Chem. 4

(2013) 277.

[8]   J. Meshram, P. Ali, V. Tiwari, Green Chem. Lett. Rev. 3 (2010) 195.

[9]   D. Kumar, M. Sonawae, B. Pujala, V.K. Jain, A.K. Chakraboti, Green Chem. 15 (2013) 2872.

[10] A. Mobinikhaled, A.K. Amiri, Lett. Org. Chem. 10 (2013) 764.

[11] C.S. Reddy, A. Srinivas, A. Nagaraj, Chem. Pharm. Bull. 57 (2009) 685.

[12] A. Shaabani, M. Seyyedhamzeh, A. Maleki, F. Rezazadeh, Appl. Catal. A: Gen. 358 (2009) 146.

[13] A. Maleki, M. Aghaei, Ultrason. Sonochem. 38 (2017) 585.

[14] A. Maleki, R. Taheri-Ledari, J. Rahimi, M. Soroushnejad, Z. Hajizadeh, ACS Omega 4 (2019) 10629.

[15] A. Maleki, R. Firouzi-Haji, P. Farahani, Org. Chem. Res. 4 (2018) 86.

[16] J. Safaei-Ghomi, F. Eshteghal, H. Shahbazi-Alavi, Ultrason. Sonochem. 33 (2016) 99.

[17] J. Safaei-Ghomi, S. Paymard-Samani, S. Zahedi, H. Shahbazi-Alavi, Z. Naturforsch. 70 (2015) 819.

[18] M. Shekouhy, R. Kordnezhadian, A. Khalafi Nezhad, Org. Chem. Res. 4 (2018) 1.

[19] R. Ranjbar-Karimi, H. Azizi, Org. Chem. Res. 3 (2017) 132.

[20] P. Cintas, Ultrason. Sonochem. 28 (2016) 257.

[21] K.S. Ojha, T.J. Mason, C.P. O'Donnell, J.P. Kerry, B.K. Tiwari, Ultrason. Sonochem. 34 (2017) 410.

[22] M. Esmaeilpour, J. Javidi, F. Dehghani, F.N. Dodeji,

[23] B. Banerjee, Ultrason. Sonochem. 35 (2017) 15.

[24] D. Heyl, E. Rikowski, R. Hoffmann, J. Schneider, W. Fessner, Chem. Eur. J. 16 (2010) 5543.

[25] A.J. Waddon, E.B. Coughlin, Chem. Mater. 15 (2003) 4555.

[26] J. Safaei-Ghomi, H. Shahbazi-Alavi, P. Babaei, Z. Naturforsch. 71 (2016) 849.

[27] J. Safaei-Ghomi, H. Shahbazi-Alavi, P. Babaei, H. Basharnavaz, S.G. Pyne, A.C. Willis, Chem. Heterocycl. Comp. 52 (2016) 288.

[28] J. Safaei-Ghomi, S. Nazemzadeh, H. Shahbazi-Alavi. Catal. Commun. 86 (2016) 14.

[29] F.A. Tameh, J. Safaei-Ghomi, M. Mahmoudi-Hashemi, H. Shahbazi-Alavi, RSC Adv. 6 (2016) 74802.

[30] U. Dittmar, B.J. Hendan, U. Flörke, H.C. Marsmann, J. Organomet. Chem. 489 (1995) 185.

[31] D.R. do Carmo, D.R. Silvestrini, T.F.S. da Silveira, L.R. Cumba, N.L.D. Filho, L.A. Soares, Mater. Sci. Eng., C. 57 (2015) 24.

[32] D.S. Fernandes, V.A. Maraldi, N.L. Dias Filho, D.R. do Carmo1, Silicon 11 (2019) 1131.

[33] Y. Chen, L. Feng, S.M. Sadeghzadeh, RSC Adv. 10 (2020) 19553.

[34] T. Previtera, M. Basile, M.G. Vigorita, G. Fenech, F. Occhiuto, C. Circosta, R.C. de Pasquale, Eur. J. Med. Chem. 22 (1987) 67.

[35] V.V. Kouznetsov, D.F. Amado, A. Bahsas, J. Amaro-Luis, J. Heterocyclic Chem. 43 (2006) 447.

RSC Adv. 5 (2015) 26625.